

Cite this: *J. Mater. Chem. A*, 2018, 6, 1671

# Effect of pressure on the gasification of dodecane with steam and supercritical water and consequences for H<sub>2</sub> production†

Ana M. Sanchez-Hernandez,<sup>id</sup> Nicolas Martin-Sanchez,<sup>id</sup> M. Jesus Sanchez-Montero,<sup>id</sup> Carmen Izquierdo<sup>id</sup> and Francisco Salvador<sup>id</sup>\*

Supercritical water (SCW) is widely known to be a powerful gasifying agent, but the supercritical gasification of linear paraffins is a method whose ability to produce H<sub>2</sub> has not been studied significantly. Herein, an analysis of the gasification of dodecane, a representative diesel compound, with steam and SCW and the ability of the method to produce H<sub>2</sub> under different pressures is reported. In this study, the broadest pressure (1–500 bar) and temperature (550–800 °C) ranges ever studied in this field are covered. We found that a fraction of the short-chain hydrocarbons generated in the thermal cracking of dodecane are turned into polycyclic aromatic compounds and phenol, compounds that hinder gasification. These reactions become more significant as steam at atmospheric pressure is progressively compressed up to SCW at 500 bar; consequently, steam gasification is faster than supercritical gasification. A gasification mechanism that gathers all of the possible pathways is proposed. Despite the slow gasification kinetics in SCW, a pressure slightly above the critical point (250 bar) is the most efficient to produce H<sub>2</sub>. At this pressure, the long reaction times related to the high SCW density allow a significant amount of CH<sub>4</sub> and CO to be reformed into H<sub>2</sub>; however, further compression is not recommended because gasification is significantly slowed down and H<sub>2</sub> production decreases.

Received 2nd November 2017  
Accepted 2nd January 2018

DOI: 10.1039/c7ta09659c

rsc.li/materials-a

## 1. Introduction

H<sub>2</sub> is one of the main alternatives to fossil fuels thanks to its energetic potential and its environmentally friendly nature. However, the storage and transport of H<sub>2</sub> has resulted in technical problems. The *in situ* generation of H<sub>2</sub> arises as a solution to this problem. Besides the use of H<sub>2</sub> as a fuel for internal combustion engines, using H<sub>2</sub> in fuel cells is the main application of *in situ* production. These cells are electrochemical devices able to turn the chemical energy stored in a fuel into electricity directly.<sup>1</sup> This is an attractive way to produce energy because fuel cells fueled by H<sub>2</sub> have high energy efficiencies and only generate water as a waste product. Proton-exchange membrane fuel cells (PEMFCs) and solid-oxide fuel cells are the most common fuel cells that use H<sub>2</sub>. An efficient H<sub>2</sub> production method is required for these applications, and, for this reason, hydrocarbons with high hydrogen densities are used as fuels. Some liquid hydrocarbons, such as gasoline and jet fuel, fulfill this requirement, but diesel stands out among

them because of its high hydrogen density. Diesel fuel is a complex mixture of hydrocarbons that contains sulfur compounds and a noticeable amount of polycyclic aromatic hydrocarbons (PAHs), which account for about 18 wt% of the mixture.<sup>2</sup> However, linear paraffins are the main fraction, and dodecane is the most representative.

Dodecane (or any another hydrocarbon) can be transformed into H<sub>2</sub> through several reforming processes such as steam reforming, partial oxidation, and autothermal reforming.<sup>2</sup> Steam reforming at atmospheric pressure uses metal-based catalysts, usually Ni. The employed catalysts result in H<sub>2</sub> concentrations of up to 70% and the complete gasification of dodecane;<sup>3–9</sup> however, temperatures above 800 °C are required. The most important drawback related to catalytic steam reforming is the deactivation of the catalyst because of carbon deposition, as well as sulfur poisoning, when real diesel is gasified.<sup>1,2,10</sup> The use of noble metals such as Pt, Rh, or Ru and other catalytic species such as K, Ce, Co, or Sr is a common solution to avoid these problems. Consequently, the catalysts consist of a support (*e.g.*, Al<sub>2</sub>O<sub>3</sub>) that contains two<sup>8–10</sup> or even three catalytic species.<sup>3–6</sup> Despite the use of these expensive materials, ultimately, the catalysts are deactivated and lose efficiency. Furthermore, CO is the main product of steam reforming, and CO poisons the electrodes employed in PEMFC cells. Hence, CO must be removed from the gas mixture produced before the H<sub>2</sub> can be used as a fuel for these cells.

Dpto. Química Física, Facultad de Ciencias Químicas, Universidad de Salamanca, Plaza de la Merced, s/n 37008 Salamanca, Spain. E-mail: anamsh@usal.es; nicolas\_martin@usal.es; chusan@usal.es; misiego@usal.es; salvador@usal.es; Tel: +34 677549970

† Electronic supplementary information (ESI) available. See DOI: 10.1039/c7ta09659c

The gasification of dodecane with supercritical water (SCW) is an attractive alternative to catalytic steam reforming. The organic compound dodecane turns into gases so SCW will be able to dissolve all the involved species; the mass transfer limitations will be lessened because of the presence of a unique homogeneous phase. In addition, SCW has been shown to be a more powerful reacting agent than steam in the gasification of other organic compounds.<sup>11</sup> Thanks to the unique properties of supercritical fluids, the reaction rate of gasification in SCW may be faster than those in steam; the reaction temperature would be reduced, catalysts will not be necessary and the idea of *in situ* H<sub>2</sub> production in small and compact facilities would be reinforced.

Despite the potential of this technique, only a few studies have been published about the supercritical gasification of intermediate-molecular-weight linear<sup>12–15</sup> or branched<sup>16–19</sup> hydrocarbons or real mixtures (diesel, gasoline or jet-fuel<sup>14,20,21</sup>); and, to the best of our knowledge, there exists just one work that has investigated the supercritical gasification of dodecane.<sup>19</sup> These works have focused on the study of the effects of the temperature, the hydrocarbon–water ratio, and the reaction time on gasification. Scant attention has been paid to the effect of pressure on the supercritical gasification of linear hydrocarbons. In fact, pressure ranges wider than 70 bar have not been investigated,<sup>12,13</sup> pressures above 250 bar have not been explored and, as far as we know, no work has compared atmospheric pressure steam and supercritical gasification.

The mechanism that controls the gasification has not been analyzed in depth either. It is generally accepted that supercritical gasification follows the same pathways as steam gasification; that is, hydrocarbons are mainly converted into gas through two endothermic reactions when steam is the gasifying agent. The first reaction is a thermal cracking caused by the high temperatures employed. The thermal cracking is explained by the model proposed by Rice and Herzfeld,<sup>22</sup> which was later updated by Benson and De More.<sup>23</sup> The model describes a radical chain process involving the rupture of the original hydrocarbons and the generation of low-molecular-weight compounds. The second reaction involved is the direct reforming of dodecane by water, eqn (1), whose standard reaction enthalpy,  $\Delta H_{25^\circ\text{C}}^0$ , and standard Gibbs free energy of reaction,  $\Delta G_{25^\circ\text{C}}^0$ , are +1866.5 and +1047.5 kJ mol<sup>-1</sup>, respectively.



The formed CO can be reformed by steam in the water–gas shift reaction, eqn (2), whose  $\Delta H_{25^\circ\text{C}}^0$  and  $\Delta G_{25^\circ\text{C}}^0$  are -41.1 and -28.6 kJ mol<sup>-1</sup>, respectively.



This work reports the gasification of dodecane, a hydrocarbon representative of diesel, with steam and SCW in the widest pressure range ever assayed in this field, from 1 to 500 bar. The use of such a wide range allows us to highlight the differences between the gasification with water in different states of matter. The effects of other parameters on the

gasification (temperature, dodecane–water ratio, and reaction time) are also analyzed. An in-depth analysis of the gasification mechanism and a comparison of the viability of H<sub>2</sub> production by supercritical gasification in comparison with the classical steam gasification are also reported.

## 2. Experimental section

### 2.1. Gasification

Fig. 1 shows the schematic of the installation used for the gasification experiments.

A 17 cm<sup>3</sup> internal volume tubular Hastelloy reactor was introduced into an electric furnace, where it was heated to the reaction temperature. A stream of water pumped by an HPLC ChromTech UHP 1500 pump passed through a preheater before reaching the gasification reactor. Once the desired temperature was attained, the dodecane began to be pumped by an HPLC LabAlliance Series 1500 pump and it was mixed with the stream of water preheated to the gasification temperature at the entrance of the reactor. Dodecane (purity of >99.8%) was purchased from Sigma-Aldrich and used as received. The stream leaving the reactor went through a heat exchanger, where it was cooled to ambient temperature, and a filter. Next, the stream was discharged through an Equilibar H10P Series Precision Back Pressure Regulator, which was used to control the gasification pressure. Once the stationary regime was attained, the process was maintained for 60 min to assess the stability of the reaction. After that period of time, the dodecane flow was stopped and the water flow was maintained for 30 min to remove any pollutant deposited on the reactor. The reaction time of each assay was calculated by approaching the density of the mixture to that of pure water at the same pressure and temperature. All the assays were carried out under laminar regime conditions (70 < Re < 880). The analyzed pressure and temperature ranges spread from 1 to 500 bar and 550 to 800 °C, respectively.

wt% is defined as follows, eqn (3):

$$\text{wt}\% = \left( \frac{\text{dodecane mass flow feeding}}{\text{dodecane mass flow feeding} + \text{water mass flow feeding}} \right) \times 100 \quad (3)$$

The analyzed wt% range spread from 0.3 to 3.0%.

### 2.2. Analysis of the produced gaseous stream

The flow, composition and concentration of the produced gases were analyzed. The gases were separated using a liquid–gas separator and passed through a cool trap at -20 °C, to retain the remaining humidity, and a thermostat at 30 °C, until they reached two six-way valves connected in series. The first valve was used to analyze the H<sub>2</sub>, CO, CO<sub>2</sub> and CH<sub>4</sub> concentrations in an Omnistar GSD 300 mass spectrometer. A Teknokroma permanent gases & light hydrocarbons TR-GC1102010 (length = 1 m; OD = 1/8"; tube wall thickness = 2.1 mm)

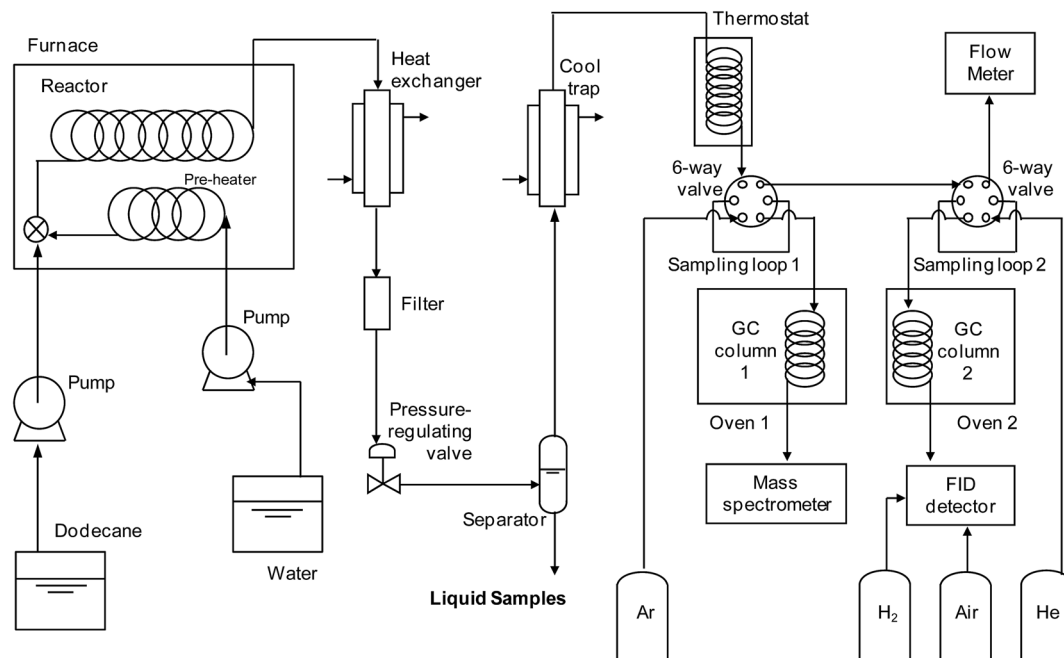


Fig. 1 Schematic of the installation used for the gasification experiments.

chromatographic column was placed between the six-way valve and the mass spectrometer. The column separated the light species from hydrocarbons, thus avoiding that hydrocarbons bigger than  $\text{CH}_4$  interfered in the analysis of  $\text{CO}$  ( $m/z = 28$ ),  $\text{CO}_2$  ( $m/z = 44$ ) and  $\text{CH}_4$  ( $m/z = 16$ ). The column was introduced in an oven and the following temperature program was used: an initial temperature of  $175\text{ }^\circ\text{C}$  maintained for 10 min, followed by a heating at  $25\text{ }^\circ\text{C min}^{-1}$  to  $325\text{ }^\circ\text{C}$ , which was finally maintained for 10 min. Ar was used as carrier gas. The second valve was used to analyze  $\text{CH}_4$ , ethane, ethylene, acetylene, propane, propylene, and butane concentrations in a Shimadzu GC-2010 Plus gas chromatograph with a  $\text{H}_2$  flame ionization detector. An Agilent HP-Plot/Q (length = 30 m; ID = 0.32 mm; thick layer of 20 micron) chromatographic column was used, with He as carrier gas. The column was introduced in an oven and the following temperature program was used: an initial temperature of  $60\text{ }^\circ\text{C}$  maintained for 3 min, followed by a heating at  $20\text{ }^\circ\text{C min}^{-1}$  to  $210\text{ }^\circ\text{C}$ , which was finally maintained for 9.5 min.

The sum of ethane, ethylene, and acetylene concentrations is shown as  $\text{C}_2$ . The sum of propane and propylene concentrations is shown as  $\text{C}_3$ . The simultaneous analysis of  $\text{CH}_4$  concentrations in the mass spectrometer and the chromatograph allow using  $\text{CH}_4$  as a pattern to calculate the relative concentration of all of the species in the global mixture. The gas concentrations were measured twice in each assay. In all of the assays, the concentration did not change once the stationary regime had been attained.

The exit of the second valve was connected to a Resteck Pro-Flow 6000 electronic flowmeter to measure the gas flow generated continuously.

The carbon gasification efficiency (CGE), eqn (4), is calculated from the characterization of the gaseous effluent:

$$\text{CGE (\%)} = \left( \frac{\text{carbon moles in the gas effluent}}{\text{carbon moles in the reactor feeding}} \right) \times 100 \quad (4)$$

where the carbon moles in the gas effluent are calculated using the molar flows of  $\text{CO}$ ,  $\text{CO}_2$ ,  $\text{CH}_4$ ,  $\text{C}_2$ ,  $\text{C}_3$  and butane. The carbon moles in the reactor feeding are calculated based on the molar flow of dodecane fed to the reactor.

The efficiency of  $\text{H}_2$  production is evaluated through  $\text{H}_2$  gas yield, which is defined as follows, eqn (5):

$$\text{H}_2 \text{ gas yield} = \frac{\text{H}_2 \text{ moles in the gas effluent}}{\text{dodecane moles in the reactor feeding}} \quad (5)$$

The same definition is used for the rest of species contained in the gas effluent.

### 2.3. Analysis of the produced liquid stream

In each assay, a liquid sample was taken from the separator to subsequently analyze its composition. These samples were analyzed by gas chromatography coupled to mass spectrometry (GC-MS). More details related to this procedure are described in the ESI.†

## 3. Results

Three different types of products were generated in the experiments: gaseous products, products contained in the aqueous reactor effluent, and other products that formed a carbonized solid residue or char. The presence of char was observed during the periodic cleaning of the reactor as small carbonized particles retained in the filter. The installation used herein hindered the measurement of the amounts of char formed under

different reaction conditions although a greater formation of char was observed as wt% and pressure were increased.

Two types of compounds were detected in the GC-MS analysis of the aqueous effluent: phenol and PAHs (naphthalene, phenanthrene, fluoranthene, and indene). The areas of the peaks associated with PAHs have been integrated in a unique area to make the interpretation of the results easier. The GC-MS analysis did not detect the presence of dodecane. The  $m/z$  spectra and the chromatographic analysis revealed that, besides  $H_2$ ,  $CO$ ,  $CO_2$ ,  $CH_4$ , and low molecular-weight hydrocarbons, phenol was also contained in the gaseous effluent. This result meant that phenol was distributed between the gaseous and liquid effluents. The amount of phenol contained in the gaseous effluent was analyzed from its peak area in the chromatographic analysis. The amount of phenol contained in the gas was not significant compared to that in the liquid. Thus, phenol was not included in the calculation of the relative concentrations of the species contained in the gas either in the calculation of CGE.

### 3.1. Effect of temperature on gasification

Fig. 2 shows the effect of temperature on CGE in the gasification of a 0.75 wt% dodecane–water mixture at 50 bar for 5 s.

CGE rose noticeably as the mixture was heated from 500 (about 9%) to 600–650 °C (about 55%). CGE continued to rise above 650 °C, but the acceleration of the gasification was milder than at low temperatures. It was necessary to increase the gasification temperature to 800 °C to convert 90% of the dodecane into gas in this brief reaction time. This trend is explained by the effect of the Gibbs free energy,  $\Delta G^0$ , on the equilibrium constant of reactions,  $K$ , eqn (6):

$$K(T) = \exp\left[-\frac{\Delta G^0(T)}{RT}\right] \quad (6)$$

According to eqn (6),  $K$  of endothermic reactions ( $\Delta H^0 > 0$ ) increases when the reaction temperature is increased. Further information about this dependence can be found in the ESI.† The achieved CGEs increased as the gasifying fluid was heated

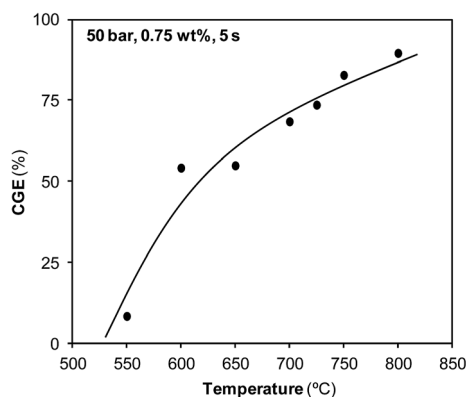


Fig. 2 Effect of temperature on CGE in the gasification of a 0.75 wt% dodecane–water mixture at 50 bar for 5 s.

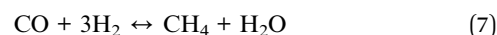
because both the thermal cracking reaction and the reforming reaction are endothermic.

Fig. 3 shows how the concentration of the species contained in the gaseous effluent evolved as dodecane was gasified at different temperatures.

At the lowest temperature investigated (550 °C), dodecane was already being gasified, but the gaseous effluent was exclusively formed of hydrocarbons.  $C_2$  and  $C_3$  hydrocarbons were found to be the most abundant. Fig. 3 points that the water reforming reaction did not occur at 550 °C (*i.e.*,  $CO$ ,  $CO_2$ , and  $H_2$  were not produced) because of its strong endothermic nature. Despite not being the aim of this investigation, Fig. 2 and 3 show that other alternatives exist for the upgrading of dodecane. The long-chain liquid hydrocarbons can be turned into low molecular-weight gaseous hydrocarbons with a greater calorific power than dodecane. Despite the energy savings that low-temperature gasification provides, this alternative has two drawbacks. First, those hydrocarbons are mainly obtained at 550–600 °C, and CGE is not very high at these temperatures; consequently, the production of hydrocarbons will be low. Secondly, olefins, especially ethylene, have been proven to be promoters of char formation.<sup>24–27</sup> The formation of char not only implies a reduction in the amount of hydrocarbons generated but also hinders the technical viability of the process.

$C_2$ ,  $C_3$ , and butane concentrations diminished as the system was heated, until they finally disappeared. The heavier hydrocarbons disappeared at lower temperatures.  $CH_4$  concentration increased with gasification temperature when heating from 550 to 650 °C, then remained almost constant, describing a plateau between 650 and 750 °C, and finally decreased above 750 °C. This trend confirms that the hydrocarbons generated in the thermal cracking are intermediate compounds of a reaction mechanism with several consecutive steps. Dodecane was progressively cracked into further light hydrocarbons as the temperature increased. Once a high enough temperature had been attained, the produced hydrocarbons began to be reformed. Fig. 3 shows that this temperature was about 600–650 °C for these specific reaction conditions. The concentrations of the reforming products ( $CO$ ,  $CO_2$ , and  $H_2$ ) increased as the gasifying fluid was heated above that temperature.

If the evolution of gas yields is analyzed instead of concentrations (see ESI†),  $CH_4$  gas yield is observed to increase with temperature over the whole temperature range, as reported by other authors who have explored narrower ranges than us.<sup>16,19</sup> This trend may be attributed to the production of  $CH_4$  in the methanation equilibrium, eqn (7), whose  $\Delta H_{25^\circ C}^0$  and  $\Delta G_{25^\circ C}^0$  are  $-206.2$  and  $-141.2$   $\text{kJ mol}^{-1}$ , respectively.



However, it does not seem probable that  $CO$  is hydrogenated to produce  $CH_4$  and water at high temperatures. According to eqn (6),  $K$  of exothermic reactions decreases with temperature. Furthermore, there is a large excess of water (which acts as a product in eqn (7)) in the system.

This result must be caused by the acceleration of the gasification process with temperature. That is, as the temperature

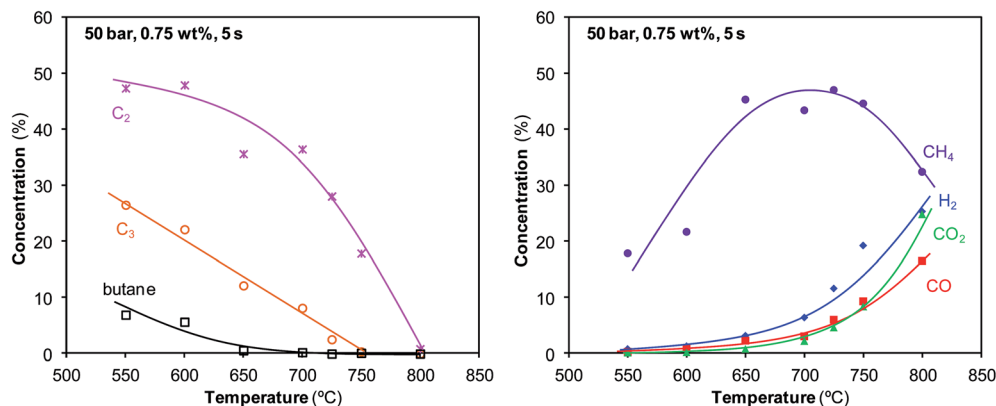


Fig. 3 Evolution of the concentrations of the species contained in the gaseous effluent with the reaction temperature.

was increased, the production of gas increased, and the  $\text{CH}_4$  gas yield also increased. The gas yield of a species will only decrease with temperature when its concentration in the gas phase diminishes noticeably, as happened in our study with butane,  $\text{C}_3$ , and  $\text{C}_2$  (see ESI†).

Fig. 4 shows the influence of temperature on the amounts of phenol contained in the liquid and gaseous effluents and the PAHs contained in the liquid effluent.

The amounts of phenol contained in the liquid and gaseous effluents were closely related. Both increased with temperature, reaching a maximum at 700–725 °C and then they decreased. The PAHs show the same trend. Phenol and PAHs seem to be progressively formed as both the temperature and CGE increased, but a temperature was reached above which the formed products began to be consumed, until they almost disappeared at 800 °C. More information about this topic is collected in the following section.

### 3.2. Effect of reaction time and pressure on gasification

Fig. 5a shows the effect of reaction time and pressure on CGE in the gasification of a 0.5 wt% dodecane–water mixture at 750 °C.

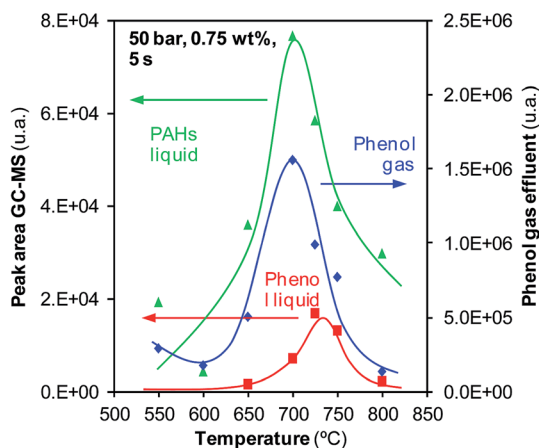


Fig. 4 Effect of temperature on the amounts of phenol and PAHs contained in the gaseous and liquid effluents.

At intermediate pressures of 50 and 150 bar, CGE increased rapidly and followed an almost linear trend as the reaction progressed. At 500 bar, the reaction behaved in the same way for the first reaction times investigated. However, as the reaction progressed, the slope decreased and the curve finally described a plateau with a CGE value lower than 100%. At 250 bar, the slope of the curve also decreased for the final reaction times investigated and it also described a plateau, although the reached CGE was slightly higher than at 500 bar.

CGE decreased with pressure over the whole range assayed, 1–500 bar. Almost complete gasification was observed at 50 and 150 bar after 0.33 and 0.56 min, respectively; however, CGE did not reach 95% at 500 bar even after 2 min reaction. CGEs greater than 87% could not be attained at atmospheric pressure, although this pressure led to the fastest kinetics; from a practical point of view, the low density of the steam at 1 bar makes the lengthening of the reaction time extremely difficult.

SCW is more reactive than steam because of the changes that water undergoes as it is compressed. The highly ordered structure of liquid water is the result of an infinite network of hydrogen bonds; at the critical point, just a small fraction of the network is preserved, but the number of bonds increases with pressure. The changes in the number of hydrogen bonds lead to variations in the dielectric constant of water. This phenomenon implies that the interactions that exist among the water molecules and the diluted species suffer considerable changes with pressure. These interactions affect the rate constant by modifying the free energy of activation and the transmission coefficient.<sup>28</sup> The interactions that SCW establishes with certain reactants like phenol<sup>11</sup> modify the free energy of activation and the mass transmission coefficient in such a way that the reactions at supercritical conditions are faster than at steam conditions. However, Fig. 5 shows the opposite trend. To verify this behavior, the whole study was repeated at a lower temperature of 725 °C (Fig. 5b). At 725 °C and 0.1 min, the CGEs achieved at 50, 150, and 250 bar were almost the same. However, as gasification progressed, it was observed that the CGEs were lower as the gasification fluid was progressively compressed. Gasification at 500 bar was slower than gasification at lower pressures throughout the whole range of reaction

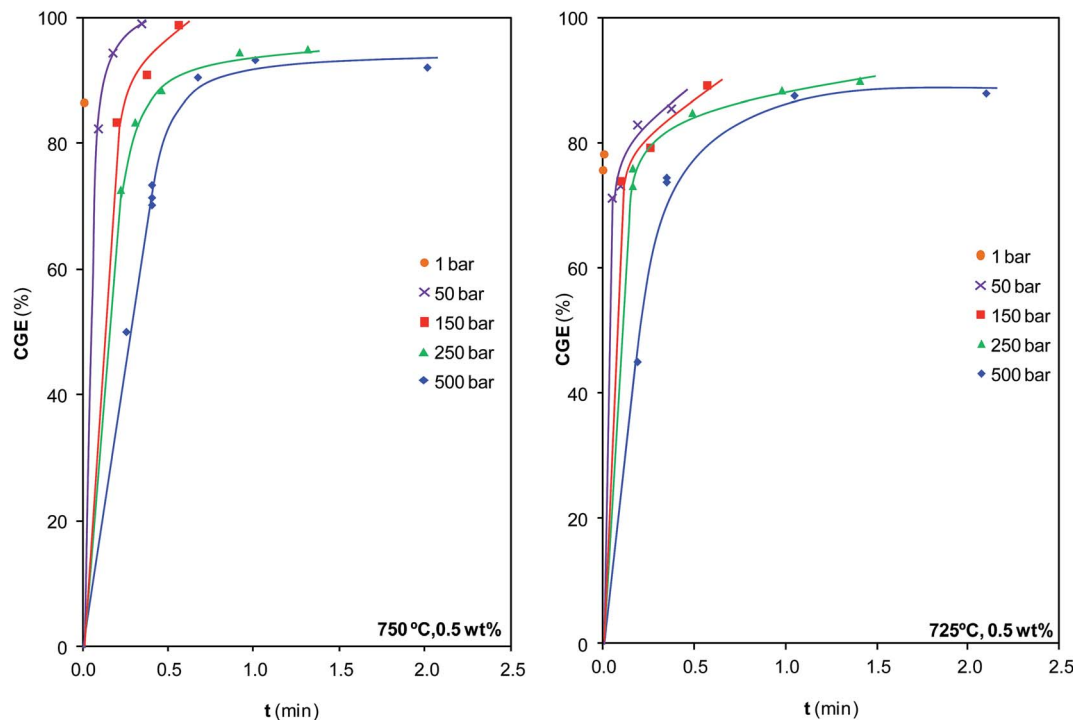


Fig. 5 Effect of reaction time and pressure on CGE at 750 °C and 725 °C.

time investigated. Consequently, we came to the same conclusion for the two temperatures investigated. The negative influence of pressure has already been suggested by the only work that has studied this topic in the gasification of a linear long-chain hydrocarbon, although the studied hydrocarbon was hexadecane and the pressure range (150–220 bar) was seven times narrower than the range studied herein.<sup>13</sup> However, the authors did not give a clear explanation for this unusual result.

The effect of pressure is the opposite of that observed when other organic compounds, such as phenol, are gasified.<sup>11</sup> The different effect of pressure on gasification may depend on the characteristics of the gasified compound, a phenomenon that has not been considered so far. This concept may explain the lack of agreement observed in several works when the effect of pressure on the gasification of organic compounds must be determined. The disagreement is especially notable when complex mixtures, such as different kinds of biomass or heavy oils, are gasified.

The analysis of the phenol and the PAHs contained in the effluents generated in gasification at 750 °C provides more information about this point, as shown in Fig. 6.

The amounts of phenol contained in the gaseous and liquid effluents were related again; both varied in the same way as the pressure changed or the reaction time increased. No phenol was generated during gasification at atmospheric pressure. At other pressures, the profile of phenol was typical of an intermediate product. This trend was quite evident at 250 and 500 bar. The concentration of phenol first increased with reaction time, suggesting that it was a reaction product. Subsequently, the phenol concentration reached a maximum and then decreased, indicating that it was consumed as a reagent in other reactions.

At 50–150 bar, the amount of generated phenol was not significant, and almost all of the formed phenol was consumed in the longest reaction times investigated. The formation of phenol increased noticeably when SCW was used as the gasifying fluid and, once inside the supercritical region, greater amounts of phenol were formed as the SCW was compressed. Phenol was not completely consumed at 250 and 500 bar because large amounts of it were formed and because of its resistance to degradation.

The PAHs contained in the liquid effluent behaved in a similar way. PAHs were formed during atmospheric pressure gasification, although the amounts were smaller than at other pressures. Their evolution with reaction time is also characteristic of intermediate compounds, and they were also further formed as the pressure increased; nevertheless, the PAHs were completely consumed at all pressures investigated. For the gasification carried out at 725 °C, similar effects of pressure and reaction time to those observed in Fig. 6 were observed (see ESI†).

When an organic molecule is contained in the bulk of SCW, the supercritical fluid can behave as a solvent or reaction medium, reagent, or, even, catalyst. Some of the reactions that organic molecules undergo when they are solved in SCW are condensation, coupling, or cyclization reactions.<sup>29,30</sup> These reactions are favored by the hydrophobic effect. The water molecules tend to bind to each other instead of binding to a hydrocarbon surface. As a consequence, nonpolar species tend to aggregate in water solution so as to decrease the hydrocarbon-water interfacial area.<sup>31</sup> This phenomenon reflects the large cohesive energy of water. Studies concerning the supercritical and subcritical gasification of different kinds of

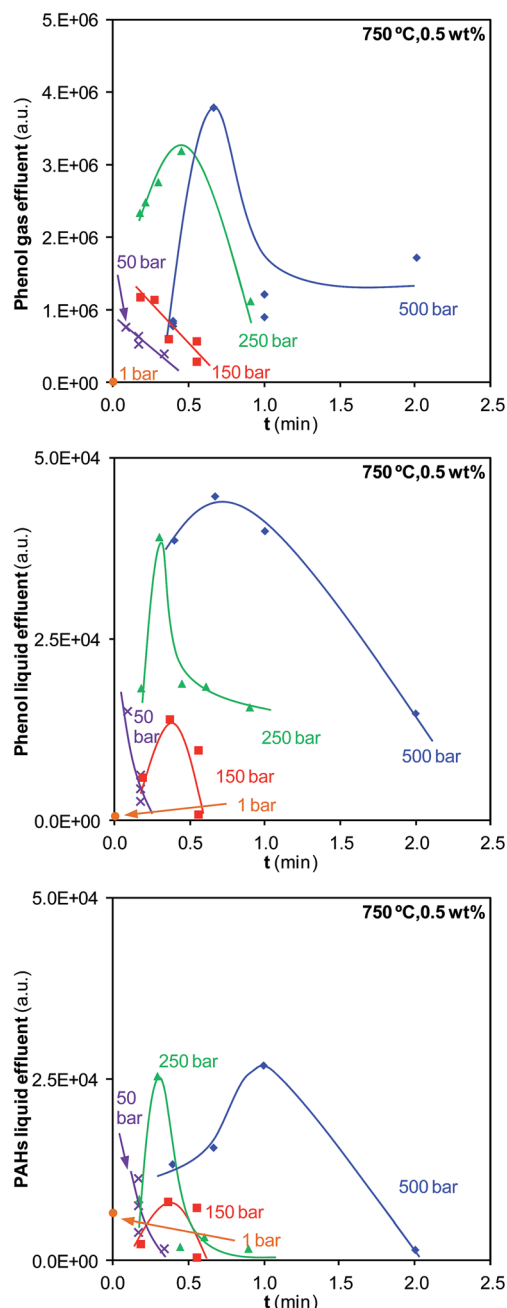


Fig. 6 Effect of pressure and reaction time on phenol and PAHs contained in the effluents generated at 750 °C.

biomass have concluded that phenols and different PAHs are formed in these reaction media as a consequence of these reactions.<sup>32–34</sup> These compounds are the main hurdle for gasifying biomass. Phenol is rather inert, and it hinders complete gasification because its degradation is difficult.<sup>35</sup> The degradation of PAHs is not as difficult as the degradation of phenol but, similar to ethylene, they are precursors for the formation of char.<sup>36,37</sup>

To date, a few works have studied in depth the compounds contained in the liquid effluents from the gasification of intermediate-molecular-weight paraffins. Depeyre *et al.*

detected the formation of monoaromatic (benzene, toluene, and styrene) and polyaromatic (naphthalene, phenanthrene, anthracene, and fluorene) compounds in the thermal steam cracking of *n*-hexadecane at atmospheric pressure and 700 °C.<sup>38</sup> They stated that these compounds could be formed (i) from the condensation of short olefins, (ii) from the addition of a diene and an olefin, or (iii) from the addition of a diene and a benzenic ring by Diels–Alder reaction followed by dehydrogenation. In fact, the Diels–Alder reaction is a very important synthetic method for the production of polycyclic ring systems.<sup>30</sup> Susanti *et al.* found phenol and different PAHs (fluoranthene and phenanthrene) in the gasification of isooctane at 763 °C and 250 bar,<sup>18</sup> but they did not explain the formation of these compounds. Alshammari and Hellgardt only detected linear paraffins and olefins in the gasification of *n*-hexadecane at 150–220 bar and 565–605 °C, with no mention of possible cyclization reactions.<sup>13</sup>

Our data suggest that the thermal cracking of dodecane yielded short-chain hydrocarbons (C<sub>2</sub>, C<sub>3</sub>, and butane) in the reaction medium, and these could act as reagents in cyclization or condensation reactions before being reformed to CO, CO<sub>2</sub>, and H<sub>2</sub>. In fact, the polymerization of liquid intermediates to cross-linked large molecules is a process that mostly occurs under high-temperature conditions, like those of SCW gasification.<sup>39</sup> Fig. 6 proves that these reactions were more relevant at high pressures. Greater amounts of difficult-to-degrade cyclic compounds were formed at supercritical pressures than at low pressures. As previously described, the number of hydrogen bonds established among the water molecules and, consequently, the cohesive energy of water, increased with pressure. The hydrophobic effect was more intense and greater fractions of short-chain hydrocarbons underwent cyclization and condensation reactions in highly pressurized SCW. These compounds slowed down the gasification, and the achieved CGEs at high pressures were low, thus explaining the results of Fig. 5. The formation of char from the olefins and PAHs, and the inability of SCW to degrade all of the formed phenol explain the incomplete gasification of dodecane under supercritical conditions. The formation of phenol and PAHs must be included when explaining the pathways involved in the gasification of dodecane. The main pathways involved in the gasification of dodecane are collected in Fig. 7.

Dodecane undergoes subsequent thermal cracking stages that progressively convert it into smaller hydrocarbons. The formed compounds become lighter as the temperature and reaction time increase. The hydrocarbons can react with water to generate the so-called reforming products, CO, CO<sub>2</sub>, and H<sub>2</sub>. The hydrocarbons can also participate in cyclization and condensation reactions that convert them into phenol and PAHs (which are precursors for char formation). Char can also be formed from the olefins contained in the reaction medium. The formed cyclic compounds can be later reformed by water. Once CO is formed, it can react with a water molecule (the water–gas shift reaction) to produce further CO<sub>2</sub> and H<sub>2</sub>. The rate and the conversion of all of these pathways depend on the gasification temperature and pressure.

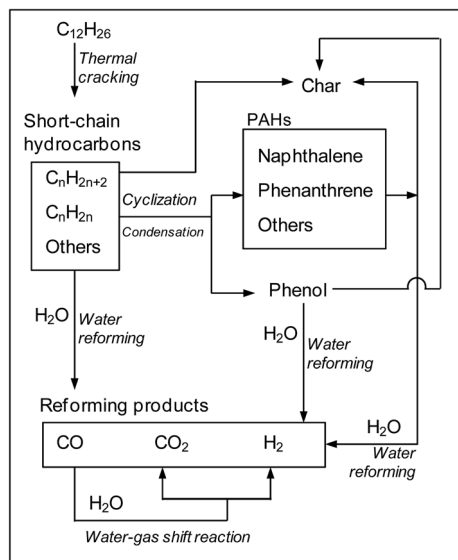


Fig. 7 Reaction pathways involved in the gasification of dodecane with steam and SCW.

The last stages of the thermal cracking produce small volatile hydrocarbons. The mixture of these hydrocarbons and the reforming products forms the gaseous effluent. Fig. 8 shows how the pressure and reaction time influence the concentration of the species contained in the gaseous effluents produced in gasification at 750 °C.

Neither butane nor  $C_3$  were detected in the gas because CGEs at 750 °C were already higher than 70%. As expected,  $C_2$  concentration decreased with time and, finally, disappeared.  $C_2$  concentration was observed to be slightly higher as the gasifying fluid was compressed, but the differences among the tested pressures were not large.  $CH_4$  is the last and the smallest hydrocarbon generated in the thermal cracking. As opposed to  $C_2$ , the pressure strongly influenced the  $CH_4$  concentration. It was high for the highest pressure (500 bar) and diminished with pressure throughout the whole range investigated. As commented in the previous section,  $CH_4$  is also an intermediate product; it is first formed in cracking reactions and later consumed in reforming reactions. Fig. 8 suggests that  $CH_4$  reforming is also faster at low pressures. Nevertheless, as far as we know, no work has been published that deals with the supercritical reforming of  $CH_4$  or the analysis of the effect of pressure on this reaction. Hence, this trend cannot be confirmed. Studies that have investigated the reforming of  $CH_4$  have focused on the synthesis of catalysts to carry out this reaction at atmospheric pressure.<sup>40,41</sup>

The effect of pressure on CO and  $CO_2$  concentrations was neither remarkable: the  $CO_2$  concentration decreased with pressure, but only slightly. CO concentration decreased with time, whereas  $CO_2$  concentration increased. This trend shows that CO, a reforming product, took part in other reactions as a reagent. It is possible that CO was consumed in reactions such as the Boudouard reaction or methanation equilibrium, but the evolution of  $CO_2$  concentration inside a system in which CO is

in contact with a strong excess of water clearly points to the water–gas shift reaction. Direct  $CO_2$  formation from the reforming of hydrocarbons, phenol, and PAHs is also a possibility, especially at high pressures. Studies concerning the gasification of carbonaceous solids with SCW demonstrate the ability of the supercritical fluid to completely oxidize carbon to  $CO_2$ .<sup>42,43</sup> This complete oxidation may also occur in this system; hence, a fraction of the  $CO_2$  may be directly generated from the reforming of short-chain hydrocarbons.

$H_2$  concentration increased almost linearly with reaction time, as expected from one of the final products of the reforming reactions.  $H_2$  concentration decreased with pressure, and its increase with time at 500 bar was slower than at lower pressures. It is noteworthy that  $CH_4$  and  $H_2$  concentrations seem to be closely related.

Fig. 5 and 8 confirm the existing relationship between CGE and the concentrations of the species contained in the gaseous effluent. As CGE increased, the concentrations of hydrocarbons decreased, and  $H_2$  and  $CO_2$  concentrations in the gas increased. The trends of the concentrations of the gases generated at 725 °C agree with those in Fig. 8 (see ESI†).

The measurement of  $H_2$  concentration allows the calculation of the  $H_2$  yield for the different conditions investigated, as listed in Table 1. This parameter clearly shows the real efficiency of the method to produce  $H_2$ . All of the experiments collected in Table 1 were carried out by pumping the same flow of water and hydrocarbon:  $1 \text{ cm}^3 \text{ min}^{-1}$  of water and  $0.007 \text{ cm}^3 \text{ min}^{-1}$  of dodecane.

The highest  $H_2$  yield was attained at 250 bar, although this pressure did not show the fastest gasification kinetics. Dodecane was not completely gasified at that pressure, but the long reaction times achieved thanks to the high density of the supercritical fluid allowed the reforming of greater amounts of  $CH_4$  and CO, and the consequent production of more  $H_2$ , than at 50–150 bar. Furthermore, the greater conversions achieved by the water–gas shift reactions under supercritical conditions (its mechanism changes from an ionic to a radical nature when compressing from steam to SCW)<sup>44–46</sup> must also be considered. The over-compression to 500 bar noticeably slowed down the gasification and reduced the  $H_2$  yield. Notably, the greatest  $H_2$  production achieved in the current investigation was just 25% of the theoretical maximum if eqn (1) and (2) are considered, that is,  $37 \text{ mol}_{H_2}/\text{mol}_{C_{12}H_{26}}$ . Longer reaction times and/or higher temperatures than those employed herein would be needed to get closer to that optimal production. SCW gasification also provides other advantages in relation to steam gasification. Fig. 8 shows that almost all of the CO can be reformed at 250 bar (final CO concentration 1.5%), whereas CO concentrations of 20% and 9% were measured at 1 and 50 bar, respectively. The use of catalysts in atmospheric pressure gasification neither reduces the CO contained in the gas; CO concentrations of about 15–20% have been reported.<sup>5,7,9</sup> The small amounts of CO generated by supercritical gasification are especially interesting because its removal and reforming will be easier, thus meeting one of the requirements for the use of the generated  $H_2$  as a fuel for PEMFCs.



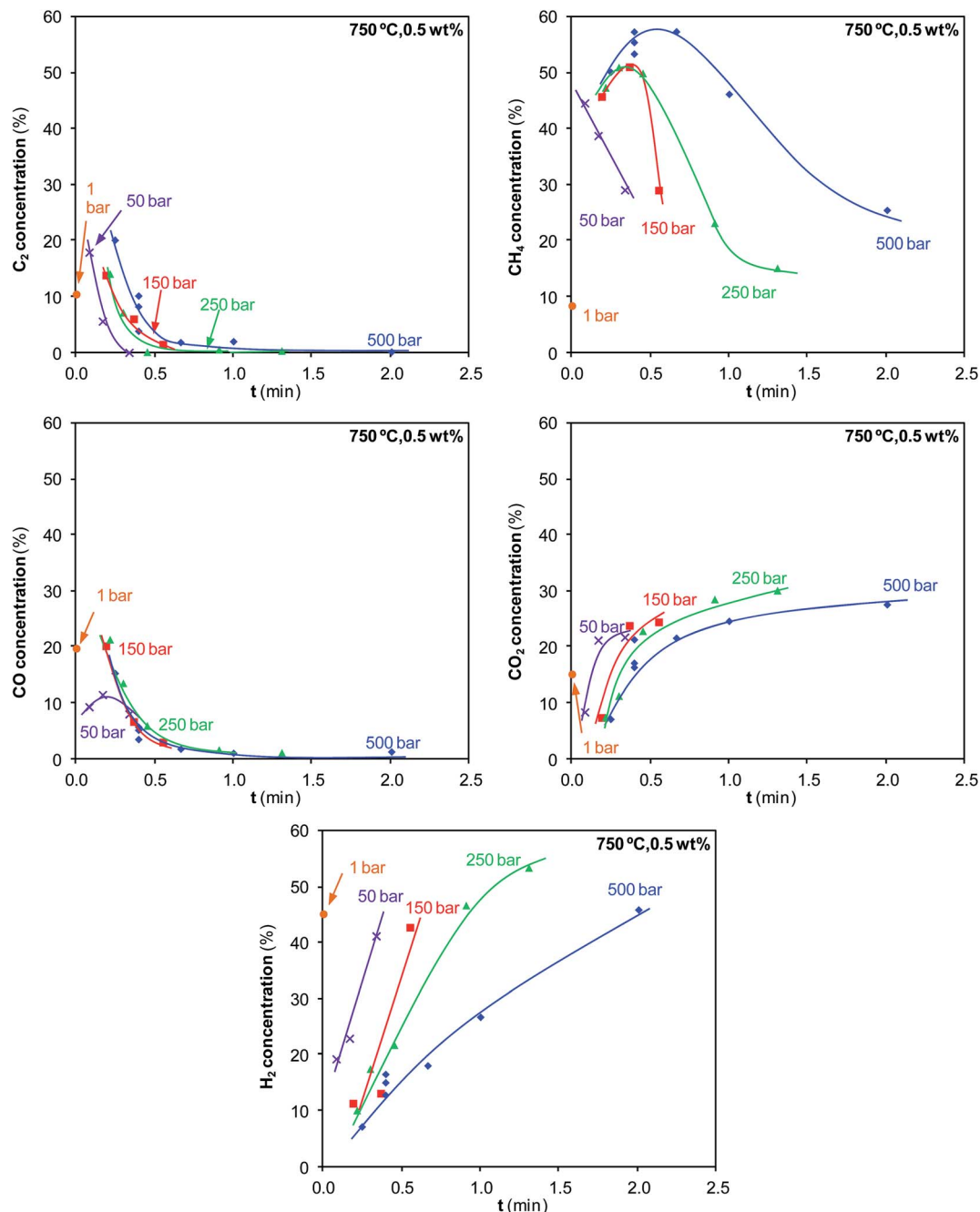


Fig. 8 Evolution of the concentrations of species contained in the gaseous effluent with pressure and reaction time.

On the other hand, it must be noted that the real mixture, diesel, contains an aromatic fraction.<sup>2</sup> The current work indicates that steam gasifies linear hydrocarbons faster than SCW,

Table 1 H<sub>2</sub> gas yields for the gasification of dodecane at 750 °C

Pressure (bar)	Reaction time (min)	H <sub>2</sub> gas yield (mol <sub>H<sub>2</sub></sub> /mol <sub>C<sub>12</sub>H<sub>26</sub></sub> )
1	0.007	5.75
50	0.17	3.15
150	0.56	8.61
250	0.91	9.72
500	2.01	9.38

but the effect of pressure on the gasification of aromatics has been shown to be the opposite.<sup>11,36</sup> Consequently, the effect that pressure has on the gasification of real mixtures cannot be accurately predicted. This topic will be analyzed in future investigations.

The data in Table 1 can be compared to the only data concerning the gasification of dodecane. Susanti *et al.*<sup>19</sup> reported a 12.2 mol<sub>H<sub>2</sub></sub>/mol<sub>C<sub>12</sub>H<sub>26</sub></sub> H<sub>2</sub> gas yield for the gasification of a 10 wt% dodecane–water mixture at 250 bar and 740 °C for 60 s. This data agrees reasonably well with our conclusions.

### 3.3. Effect of concentration under different gasification conditions

The mechanism in Fig. 7 shows the importance of phenol and PAHs on gasification. The previous results prove that the reactions that generate these products are promoted by high pressures. The formation of cyclic compounds may also be promoted by increasing the concentration of dodecane in the mixture, *i.e.*, wt%. Fig. 9 shows the influence of wt% on gasification at 725 °C and different pressure and reaction time conditions.

A high pressure (500 bar) and a low pressure (50 bar) were chosen to carry out this study. Fig. 9a shows that CGE of gasification at 50 bar for 0.18 min varied little with changing wt%. However, CGE clearly decreased with wt% in gasification at 500 bar for 1.05 min. The concentrations of the species contained in the gas evolved as expected when analyzing the evolution of CGE (see ESI†).

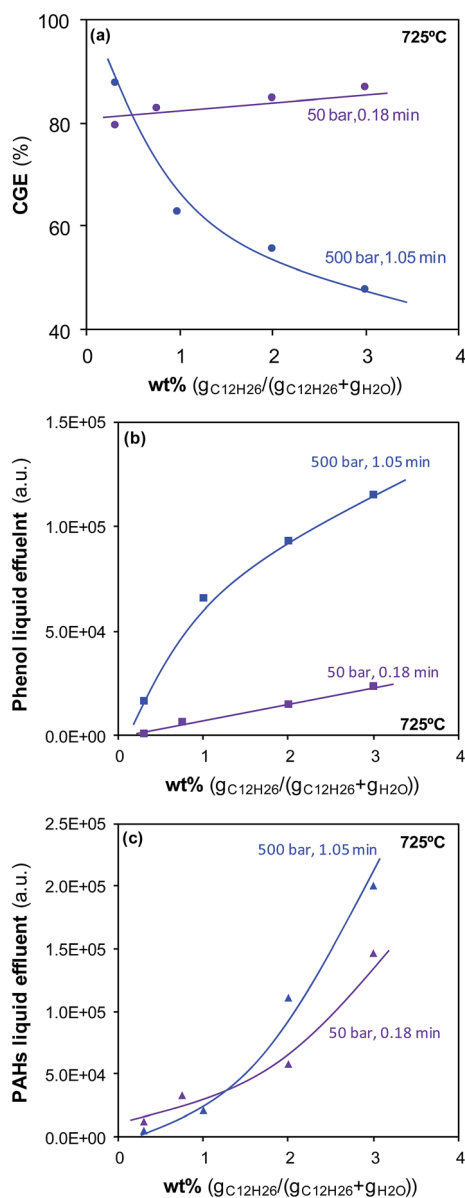


Fig. 9 Effect of wt% on gasification at 725 °C.

Fig. 9b and c show that the amounts of phenol and PAHs contained in the liquid effluent increased noticeably with increasing wt% at 500 bar. These results confirm that high pressures promoted the cyclization and condensation of linear hydrocarbons. PAHs also increased at 50 bar but this fact does not seem to affect the proportion of gasified dodecane. On the other hand, the amount of phenol in the liquid effluent after gasification at 50 bar increased slightly when the mixture contained a high concentration of dodecane. Similar conclusions were obtained when the phenol in the gas effluent was analyzed (see ESI†). That is to say, the most remarkable differences between both pressures are observed for phenol. Consequently, the formation and later consumption of phenol seem to be the factors having the strongest influence on CGE. As previously commented, the degradation of phenol is difficult and its formation as by-product in the gasification of other carbon-based materials such as lignite or glucose has been demonstrated to hinder gasification.<sup>33,34</sup> Herein, the formation of great amounts of phenol at high pressures also hinders the gasification of dodecane. The amounts of phenol formed at low pressures are small and, thus, the gasification kinetics at 50–150 bar are faster than at 250–500 bar.

## 4. Conclusions

This work shows the ability of non-catalyzed gasification with steam, subcritical water, and SCW to upgrade long-chain linear hydrocarbons. Depending on the reaction conditions some undesirable compounds such as PAHs, phenol, and char are formed. However, the selection of the gasification conditions allows (i) the complete gasification of the hydrocarbon and (ii) the maximization of H<sub>2</sub> production.

The effect of pressure on the gasification of intermediate-weight linear paraffins is reported for the first time. The lowest CGEs are attained for the highest pressures investigated. This trend is the opposite of what may be predicted according to the properties of steam and SCW. The analysis of the liquid effluent reveals that the short-chain hydrocarbons generated in the process undergo condensation and cyclization reactions, thus generating phenol and PAHs. Phenol is difficult to degrade and is the main hurdle to the complete gasification of dodecane. The formation of large amounts of phenol at high pressures makes the supercritical gasification kinetics slower than the steam gasification kinetics.

Although steam gasifies dodecane faster than SCW, low pressures do not lead to the production of the greatest amounts of H<sub>2</sub>. The long reaction times achieved in the supercritical gasification thanks to the high density of SCW allow the reforming of a high percentage of CH<sub>4</sub> and CO into H<sub>2</sub> and CO<sub>2</sub>. The over-compression of SCW to 500 bar noticeably slows down the gasification process and reduces H<sub>2</sub> production. In summary, for the conditions used in this work, a pressure slightly above the critical pressure (250 bar) leads to optimal H<sub>2</sub> production.

The effect of pressure shown herein is the opposite of that observed for the gasification of other organic compounds with different structures. This conclusion encourages continuing the

investigation in this field, focusing on different types of compounds (linear, cyclic, branched, saturated, and unsaturated) to obtain in-depth knowledge of the true effect of pressure on the gasification and upgrading of biomass.

## Conflicts of interest

There are no conflicts to declare.

## Acknowledgements

Financial support from the Spanish Ministerio de Economía y Competitividad (Project CTQ2015-64339-R) and Anticipos Fondos Feder is acknowledged.

## References

- 1 C. Song, *Catal. Today*, 2002, **77**(1–2), 17–49.
- 2 J. Bae, S. Lee, S. Kim, J. Oh, S. Choi, M. Bae, I. Kang and S. P. Katikaneni, *Int. J. Hydrogen Energy*, 2016, **41**(44), 19990–20022.
- 3 V. S. Guggilla, J. Akyurtlu, A. Akyurtlu and I. Blankson, *Ind. Eng. Chem. Res.*, 2010, **49**(17), 8164–8173.
- 4 T. Kim, K. H. Song, H. Yoon and J. S. Chung, *Int. J. Hydrogen Energy*, 2016, **41**(40), 17922–17932.
- 5 Z. Xiao, L. Li, C. Wu, G. Li and G. Liu, *Catal. Lett.*, 2016, **146**(9), 1780–1791.
- 6 Z. Xiao, C. Wu, L. Li, G. Li, G. Liu and L. Wang, *Int. J. Hydrogen Energy*, 2017, **42**(8), 5606–5618.
- 7 C. Fabiano, C. Italiano, A. Vita, L. Pino, M. Laganà and V. Recupero, *Int. J. Hydrogen Energy*, 2016, **41**(42), 19475–19483.
- 8 H. Iida, N. Onuki, T. Numa and A. Igarashi, *Fuel Process. Technol.*, 2016, **142**, 397–402.
- 9 A. Vita, C. Italiano, C. Fabiano, L. Pino, M. Laganà and V. Recupero, *Appl. Catal., B*, 2016, **199**, 350–360.
- 10 Q. Zheng, C. Janke and R. Farrauto, *Appl. Catal., B*, 2014, **160–161**, 525–533.
- 11 N. Martin-Sanchez, M. J. Sanchez-Montero, C. Izquierdo and F. Salvador, *React. Chem. Eng.*, 2017, **2**(5), 799–810.
- 12 Y. M. Alshammari and K. Hellgardt, *Int. J. Hydrogen Energy*, 2012, **37**(7), 5656–5664.
- 13 Y. M. Alshammari and K. Hellgardt, *J. Supercrit. Fluids*, 2016, **107**, 723–732.
- 14 K. Pinkwart, T. Bayha, W. Lutter and M. Krausa, *J. Power Sources*, 2004, **136**(2), 211–214.
- 15 M. Watanabe, H. Hirakoso, S. Sawamoto, T. Adschiri and K. Arai, *J. Supercrit. Fluids*, 1998, (1–3), 247–252.
- 16 B. Veriansyah, J. Kim, J. D. Kim and Y. W. Lee, *Int. J. Green Energy*, 2008, **5**, 322–333.
- 17 R. F. Susanti, B. Veriansyah, J. D. Kim, J. Kim and Y. W. Lee, *Int. J. Hydrogen Energy*, 2010, **35**(5), 1957–1970.
- 18 R. F. Susanti, A. Nugroho, J. Lee, Y. Kim and J. Kim, *Int. J. Hydrogen Energy*, 2011, **36**(6), 3895–3906.
- 19 R. F. Susanti, L. W. Dianningrum, T. Yum, Y. Kim, Y. W. Lee and J. Kim, *Chem. Eng. Res. Des.*, 2014, **92**(10), 1834–1844.
- 20 J. W. Picou, J. E. Wenzel, H. B. Lanterman and S. Lee, *Energy Fuels*, 2009, **23**(12), 6089–6094.
- 21 S. Lee, H. B. Lanterman, J. E. Wenzel and J. W. Picou, *Energy Sources, Part A*, 2009, **31**, 1750–1758.
- 22 F. O. Rice and K. F. Herzfeld, *J. Am. Chem. Soc.*, 1934, **56**(2), 284–289.
- 23 S. W. Benson and W. B. De More, *Annu. Rev. Phys. Chem.*, 1965, **16**, 397–450.
- 24 S. Yoon, I. Kang and J. Bae, *Int. J. Hydrogen Energy*, 2008, **33**(18), 4780–4788.
- 25 S. Yoon, I. Kang and J. Bae, *Int. J. Hydrogen Energy*, 2009, **34**(4), 1844–1851.
- 26 D. K. Liguras, D. I. Kondarides and X. E. Verykios, *Appl. Catal., B*, 2003, **43**(4), 345–354.
- 27 J. Comas, F. Mariño, M. Laborde and N. Amadeo, *Chem. Eng. J.*, 2004, **98**(1–2), 61–68.
- 28 N. Akiya and P. E. Savage, *Chem. Rev.*, 2002, **102**(8), 2725–2750.
- 29 G. Brunner, *Supercritical Fluid Science and Technology*, 2014, vol. 5, pp. 265–322.
- 30 N. Simsek-Kus, *Tetrahedron*, 2012, **68**(4), 949–958.
- 31 R. Breslow, *Acc. Chem. Res.*, 1991, **24**(6), 159–164.
- 32 A. Kruse, T. Henningsen, A. Sinag and J. Pfeiffer, *Ind. Eng. Chem. Res.*, 2003, **42**(16), 3711–3717.
- 33 P. T. Williams and J. A. Onwudili, *Ind. Eng. Chem. Res.*, 2005, **44**(23), 8739–8749.
- 34 H. Jin, C. Fan, L. Guo, S. Liu, C. Cao and R. Wang, *Energy Convers. Manage.*, 2017, **145**, 214–219.
- 35 A. Kruse, *Biofuels, Bioprod. Biorefin.*, 2008, **2**, 415–437.
- 36 C. M. Huelsman and P. E. Savage, *J. Supercrit. Fluids*, 2013, **81**, 200–209.
- 37 T. L. K. Yong and Y. Matsumura, *Ind. Eng. Chem. Res.*, 2013, **52**(26), 9048–9059.
- 38 D. Depeyre, C. Flicoteaux and C. Chardaire, *Ind. Eng. Chem. Process Des. Dev.*, 1985, **24**(4), 1251–1258.
- 39 D. Castello, A. Kruse and L. Fiori, *Chem. Eng. Res. Des.*, 2014, **92**(10), 1864–1875.
- 40 S. D. Angeli, G. Monteleone, A. Giaconia and A. A. Lemonidou, *Int. J. Hydrogen Energy*, 2014, **39**(5), 1979–1997.
- 41 P. V. Laxma Reddy, K. H. Kim and H. Song, *Renewable Sustainable Energy Rev.*, 2013, **24**, 578–585.
- 42 N. Martin-Sanchez, F. Salvador, M. J. Sanchez-Montero and C. Izquierdo, *J. Phys. Chem. Lett.*, 2014, **5**(15), 2613–2618.
- 43 N. Martin-Sanchez, M. J. Sanchez-Montero, C. Izquierdo and F. Salvador, *Carbon*, 2016, **99**, 502–513.
- 44 C. F. Melius and N. E. Bergan, *Twenty-Third Symposium (International) on Combustion*, The Combustion Institute, 1990, pp. 217–223.
- 45 S. F. Rice, R. R. Steeper and J. D. Aiken, *J. Phys. Chem. A*, 1998, **102**(16), 2673–2678.
- 46 J. D. Taylor, C. M. Herdman, B. C. Wu, K. Wally and S. F. Rice, *Int. J. Hydrogen Energy*, 2003, **28**(11), 1171–1178.